

# Comparison of clear water flow and sediment flow through bottom racks using some lab measurements and CFD methodology

L. Castillo<sup>1</sup>, J. Carrillo<sup>1</sup> & J. García<sup>1</sup>

<sup>1</sup>*Department of Civil Engineering,  
Technical University of Cartagena, Spain*

## Abstract

Bottom water intake systems consist of a rack located on the stream bed, so that water passes through the rack to be collected. These structures are used in small mountain rivers with steep slopes and irregular riverbeds, in which intense sediment transport and flood flow are found. These racks are designed to derive as much water as possible with the minimum retention of solids. Some attention has been given to the occlusion of racks due to the deposition of debris over them or to the quantity of sediment that gets into the rack and is transported along the derivation channel. Nowadays what we want is to optimize this kind of intake to use them in discontinuous and torrential streams with a high concentration of sediment.

The methodology of Computational Fluid Dynamics (CFD), which is based on numerical solution of the Reynolds Averaged Navier-Stokes (RANS) equations together with turbulence models of different degrees of complexity, simulates the interaction between different fluids, such as the sediment-water two-phase flows that appear in intake systems.

This paper compares the main results obtained in clear water flow and sediment flow through a rack, using some laboratory results and CFD methodology.

*Keywords: bottom intake system, racks, lab, sediment, CFD.*

## 1 Introduction

In the design of a bottom intake system, it is necessary to consider different aspects. The efficiency of the racks depends on various factors such as the shape



of the bars, clear space between the bars (void ratio), flow approximation conditions and quantity, the angle of the rack, length, sediment rate, etc.

In theory, without taking into account the sediments, the flux over the rack is one-dimensional, the flow decreases progressively, hydrostatic pressure distribution acts over the rack in the flow direction and the energy level or the energy head are constant along the rack.

Several researchers have looked into the problem using different hydraulic models. Nosedá [1] studied the clear water flow through different racks. The racks were formed with  $T$  profile bars positioned parallel to the direction of the flow. In each test the flow collected by the rack and the longitudinal geometric profile of the flow in the centreline of the channel were measured.

Differences between measured and calculated profile values are generally found in the initial part of the rack due to the consideration of hydrostatic pressure distribution, and at the edge of the rack when friction effects are neglected (Brunella *et al.* [2]).

Righetti *et al.* [3] proposed to calculate the flow derived by the rack with the following differential equation:

$$dq(x) = C_q m \sqrt{2g(H_0 + \Delta z)} dx \quad (1)$$

where  $m$  is the void ratio,  $dx$  is the increment longitudinal in the flow direction,  $H_0$  is the total energy at the beginning of the rack,  $\Delta z$  is the vertical distance between the initial rack section and the analyzed section, and  $C_q$  is the discharge coefficient. Righetti and Lanzoni [4] propose that  $C_q \approx \sin \alpha$ , being  $\alpha$  the angle of the velocity vector of water derived with the rack plane.

Some experimental studies have found a correlation between the influence of the sediments and the flow derived by the rack (Orth *et al.* [5]). Krochin [6] proposes an increment coefficient in the long of the rack for considering the clog problems. Drobir [7] published some results for different types of sieve curves in mountain rivers. Castillo and Lima [8] have analysed and compared the formulae of several authors.

## 2 Purpose

As a result of the existence of boundary layer separations and high turbulence that make the study difficult using traditional methodologies, we considered it necessary to build a parallel numerical model in order to confirm the data obtained in physical models.

## 3 Clear water simulation

### 3.1 Physical model

An intake system has been constructed in the Hydraulic Laboratory at the Universidad Politécnica de Cartagena. It consists of a 5-meter long and 0.50-meter wide channel, a rack with different slopes, the discharge channel and the



channel to collect water discharged. The racks were made of aluminium bars and were located at the bottom of the channel.

The experiments were carried out using racks with different void ratios. The racks were built with *T* profile with the same width, but the longitudinal layout was modified to allow different spacing between them. Table 1 summarizes the geometric characteristics of each experiment that we carried out.

Table 1: Geometric characteristics of the lab experiments.

Experiment	A	B	C
Length, $L$ (m)	0.900	0.900	0.900
Bar type (mm)	T 30/25/2	T 30/25/2	T 30/25/2
Direction of the flow	Longitudinal	Longitudinal	Longitudinal
Spacing, $b_l$ (mm)	5.70	8.50	11.70
Coefficient $m = \frac{b_l}{b_l + 30}$	0.16	0.22	0.28

In each experiment, the incoming, derived and rejected flows and the longitudinal flow profile were measured.  $q_1$  is the incoming specific flow,  $q_2$  is the specific discharge flow rejected, and  $q_d$  is the specific discharge flow derived from the intake system. Table 2 shows the entrance specific flow.

Table 2: Entrance specific flow in the physical model.

N° experiment	1	2	3	4	5
$q_1$ (l/s/m)	53.8	77.0	114.6	155.4	198.3

### 3.2 Numerical model

The Computational Fluid Dynamics program allows us to simulate the interaction between different fluids as a two-phase air-water or flows with different concentrations. The program incorporates any fluid mechanical problem into its geometric configuration, providing lot of data, increased profitability, flexibility and speed which cannot be obtained with experimental procedures. However, to use it correctly, it is necessary to contrast and to calibrate it with data obtained in prototypes or physical models.

To test the hydraulic behaviour of an intake system, the experimental data measured by Nosedá [1] was used in order to model and calibrate the CFD program.

FLOW-3D uses a difference finite scheme solving the differential Navier-Stokes equations of the phenomenon in control volumes defined by the meshing of the fluid domain. The continuity and momentum Navier-Stokes equations are applied:

$$\frac{\partial u_i}{\partial x_i} = 0 \quad (2)$$

$$u_j \frac{\partial u_i}{\partial x_i} = -\frac{1}{\rho} \frac{\partial}{\partial x_i} (P \delta_{ij} + \rho \overline{u_i u_j}) \quad (3)$$

being  $P$  the dynamic pressure,  $\rho$  the flow density,  $u_i$  the  $i$  component of the local time-averaged flow velocity,  $\delta$  the Kronecker Delta function and  $\rho \overline{u_i u_j}$  the turbulence stresses.

To complement the numerical solution of Reynolds equations and average Navier-Stokes (RANS), a turbulence model has been used.

Renormalization-Group (RNG) k- $\epsilon$  model (Yakhot and Orszag [9], Yakhot and Smith [10]) has been used. This turbulence model applies statistical methods to the derivation of the averaged equations for turbulence quantities, such as turbulent kinetic energy and its dissipation rate. Generally, the RNG k- $\epsilon$  model has wider applicability than the standard k- $\epsilon$  model. In particular, the RNG model is known to describe low intensity turbulence flows and flows having strong shear regions more accurately (FLOW 3D [11]).

To simulate clean water flow, we selected the one fluid option, join the air entrainment models (fig 1).

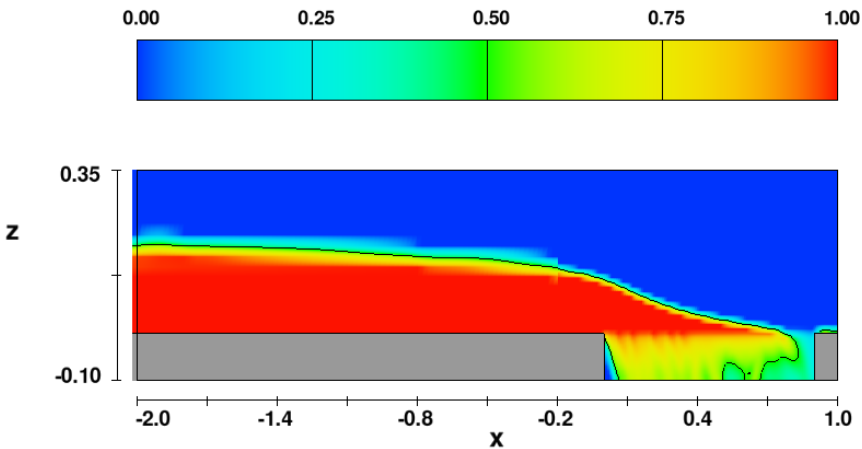


Figure 1: Fraction of fluid after 25 seconds, without sediments and  $q_1 = 155.4$  l/s/m.

The model boundary conditions correspond to the flow at the inlet, upstream and downstream levels and their hydrostatic pressure distributions. At the bottom

of the exit channel of water collected by the rack we used outflow condition due that the fact that at this boundary the hydrostatic pressure condition is not allowed.

In FLOW-3D it is only able to run transient state simulations. However it is possible to use stop criteria when the simulation reaches a steady state. The timescale is obtained at each step in order to satisfy different internal stability criteria.

For simplicity, we took into account that in the intake system all the longitudinal bars work in the same mode. For that reason, we used symmetrical conditions in the central plane of the spacing between bars (Castillo and Carrillo [12]).

We have used a mesh measuring 0.01 m long near the rack and 0.02 m in the rest of the model, using 54633 elements (fig. 2).

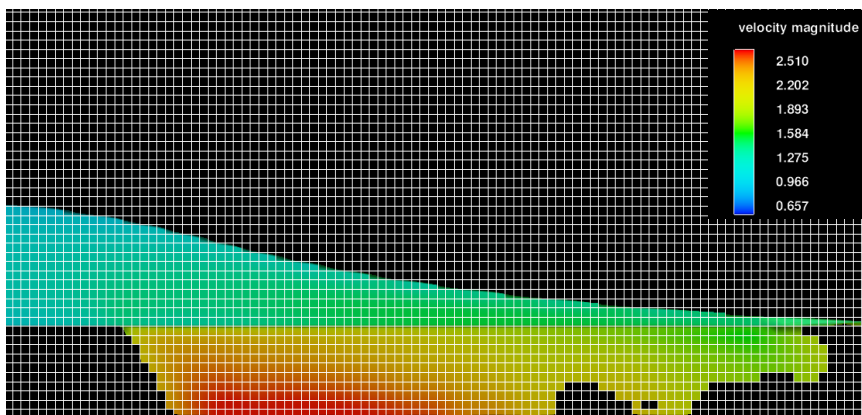


Figure 2: Detail of fluid domain geometry passing through the spacing, without sediments.

### 3.2.1 Results and discussion

In order to know the accuracy of the numerical simulations data, firstly, we compared the longitudinal flow profiles over the centre of the bar simulated with the results obtained by Nosedá [1] and UPCT laboratory.

Fig. 3 compares the depth of the longitudinal flow profiles obtained with the biggest, medium and smallest specific flows using the three methodologies, and considering spacing  $b_I = 8.50$  mm ( $m = 0.22$ ). The differences of FLOW-3D are up to 1 cm below lab results.

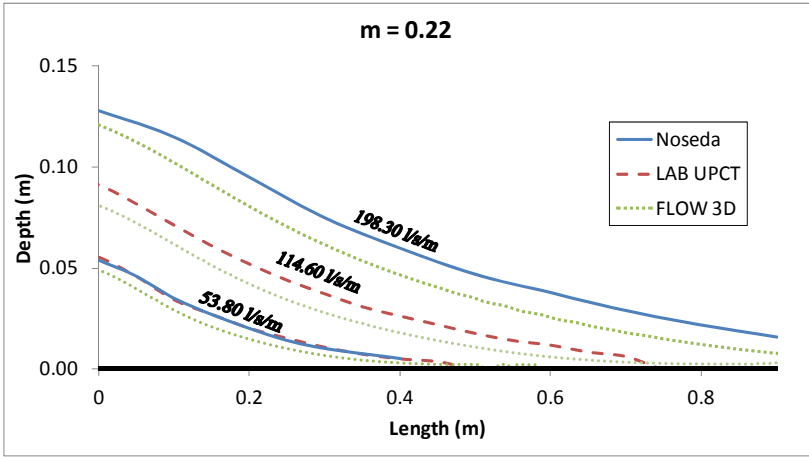


Figure 3: Flow profiles over the centre of the bar with horizontal rack,  $b_l = 8.50$  mm and  $q_l = 53.8, 114.6$  and  $198.30$  l/s/m.

Fig. 4 shows the depth water profiles considering  $b_l = 5.70$  mm ( $m = 0.16$ ). We can observe that FLOW-3D obtains profiles up to 1.5 cm below the lab measurements in the edge of the rack when the bigger specific flow is considered.

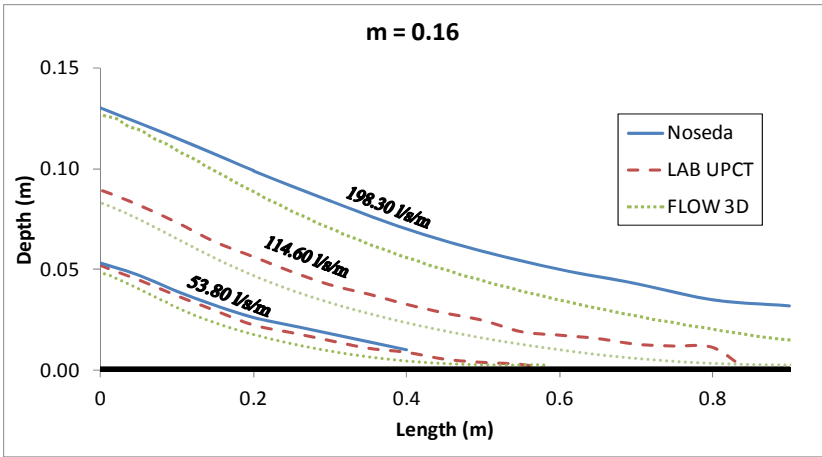


Figure 4: Flow profiles over the centre of the bar with horizontal rack,  $b_l = 5.70$  mm and  $q_l = 53.8, 114.6$  and  $198.30$  l/s/m.

After this, we compared the relation between specific flow,  $q_l$ , and specific flow derived in the intake system,  $q_d$ , for two spacing ( $b_l = 8.50$  and  $5.70$  mm). In fig. 5 we have obtained similar results with lab and Nosedá's measurements, except for  $q_l = 198.3$  l/s/m in which FLOW-3D collected more flow.



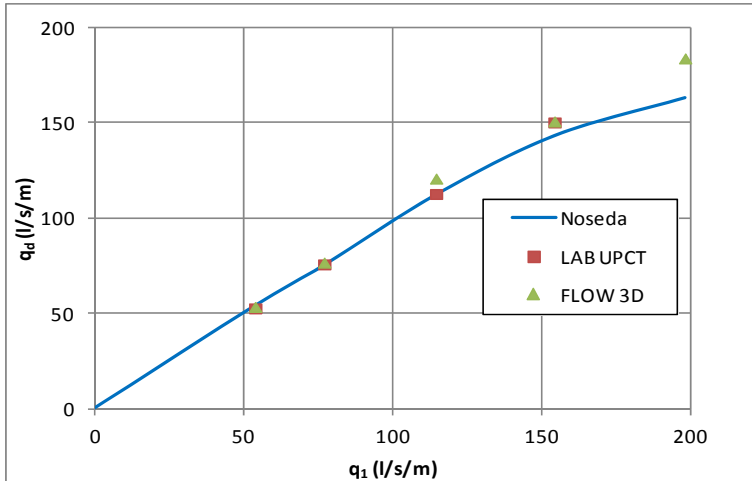


Figure 5: Derivation capacity of the intake system, with  $b_l = 8.50$  mm,  $m = 0.22$ .

Fig. 6 shows similar results in the lower flows and important differences between Noseda and UPCT results for the bigger flows.

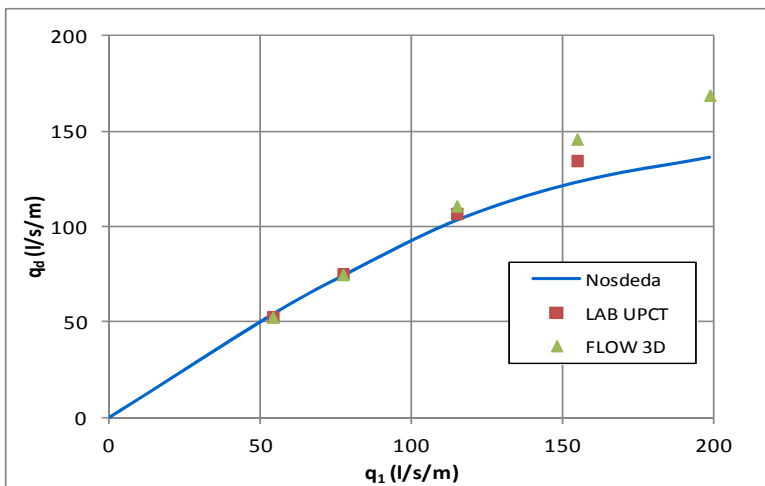


Figure 6: Derivation capacity of the intake system, with  $b_l = 5.70$  mm,  $m = 0.16$ .

Finally, we compared the angle of the velocity vector of water derived with the rack plane,  $\alpha$ , measured in the centre of the spacing between bars. Righetti *et al.* [3] obtained in their lab studies that the range of  $\sin \alpha$  is between 0.5 and 0.7, lowering with the decrease in water depth.

Fig. 7 shows the results obtained with numerical simulations using CFD programs for the specific flow  $q_1=198.30$  l/s/m and  $q_1=53.80$  l/s/m. Despite the fact that different bar settings and flows are used, you can see that the values obtained are in the same range as those shows in the lab, reducing  $\sin \alpha$  downstream as the water depth decreases.

On the other hand, there are not significant variations between the results obtained with different spacing. These results give a good overview of the values that adopt  $C_q$  coefficient along the rack.

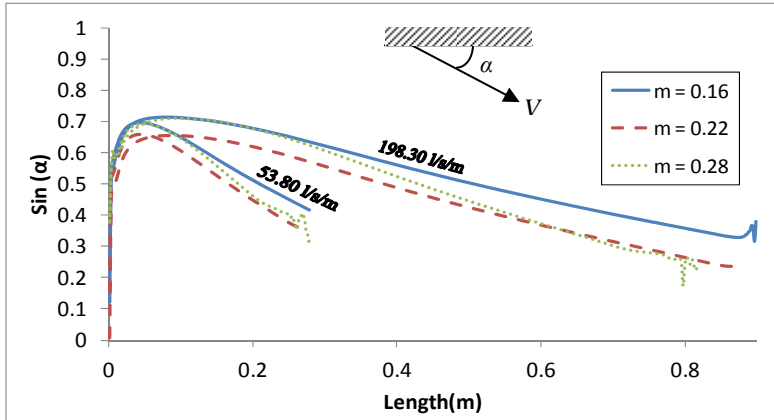


Figure 7: Variation of  $\sin(\alpha)$  in the centre of the spacing, with  $q_1$  53.8 and 198.30 l/s/m.

## 4 Sediment simulation

### 4.1 Numerical model

The sediments model considers two situations: lifting and particle transport. The first takes place at the interface between the liquid and solid surfaces and generates the transport of the particles when the effort caused by the flow exceeds a critical value, and consequently, the amount of raised particles of the ground is proportional to the shear stress. The transport component simulates the movement of the solid particles in the fluid, and additionally, the model incorporates a drive module, which is used to simulate the behaviour of solids when flowing at high concentrations. The density and viscosity of the fluid are calculated from the concentration of sediments.

### 4.2 Sediment characteristics

The characteristic diameters of the material used for the simulation was sand of  $d_{50} = 5$  mm, silt of  $d_{50} = 1 \times 10^{-2}$  mm, and a mixture of both materials in the same proportion. At the beginning of the rack, different volumetric concentrations between 1 and 10% have been simulated.



#### 4.2.1 Results and discussion

Nosedá's bars are so long that they collect almost all the water flowing over the racks. This limits the study of different sediment concentrations with lab specific flows. For this reason, the ratio between specific flow,  $q_l$ , and specific flow derived in the intake system,  $q_d$ , has been obtained considering different sediment's mixture concentration upstream of a rack of 0.50 m length.

Fig. 8 shows an example of how the silt component of the mixture 2.5% ( $30 \text{ kg/m}^3$ ) tends to be swept downstream over the bars.

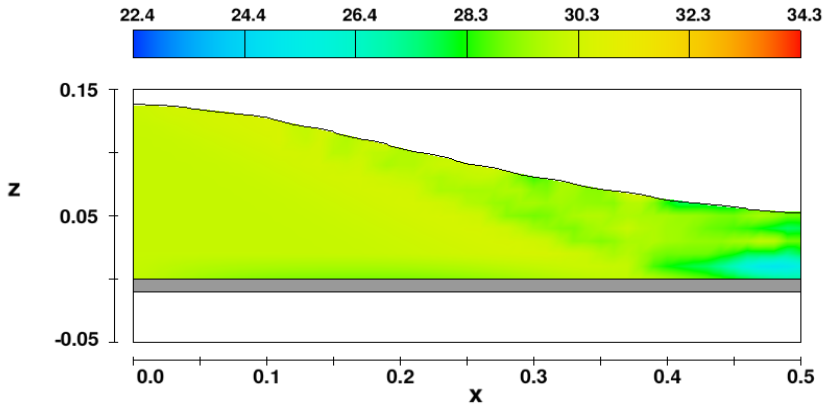


Figure 8: Silt of the mix over the bars, with  $b_l = 5.70 \text{ mm}$ ,  $m = 0.16$ ,  $L = 0.50 \text{ m}$ . Mixture sediment concentration of 5 % ( $71.25 \text{ kg/m}^3$ ).

Fig. 9 shows the sand concentration of the flow 2.5 % ( $41.25 \text{ kg/m}^3$ ). We can see that the sand tends to fall up to the first half of the rack.

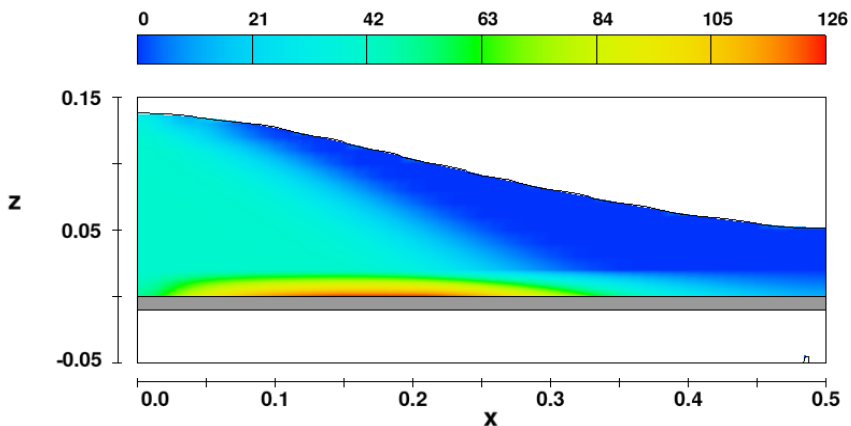


Figure 9: Sand of the mix over the bars, with  $b_l = 5.70 \text{ mm}$ ,  $m = 0.16$ ,  $L = 0.50 \text{ m}$ . Mixture sediment concentration of 5 % ( $71.25 \text{ kg/m}^3$ ).

Fig. 10 shows the results for a rack of 0.50 m and a spacing between the bars of 5.70 mm. We can see that in the case of a 10% concentration of sediment, the derived flow is reduced by almost 50% for the largest flow case in relation with the collected flow obtained with a rack with the adequate length to collect the entrain flow (198.30 l/s/m).

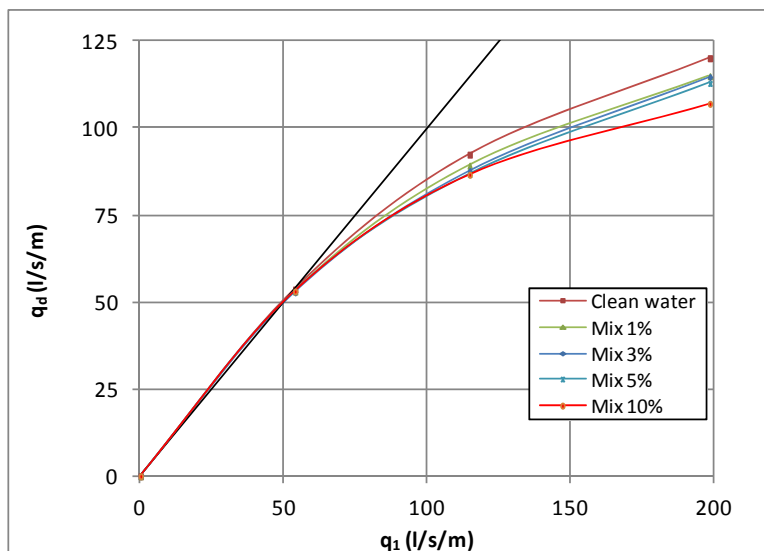


Figure 10: Derivation capacity of the intake system considering different concentrations, with  $b_f = 5.70$  mm,  $m = 0.16$ ,  $L = 0.50$  m.

## 5 Conclusions

There are different laboratory studies modelling clean water flow over racks with different bar shapes, slopes and spacing. However, there are very few studies looking at the effects of sediment on the rack behaviour.

To improve our knowledge of these structures, it is important to do more experimental studies, both physical models and prototypes, simultaneously measuring the depths, velocity and sediment rates.

In this paper we have tested the accuracy of the numeric results obtained with CFD methodology as a tool to model an intake system with clean water.

Furthermore, a numerical sediments preliminary study has been carried out before to start analyzing sediments in our lab device. Lab results will allow us to calibrate and validate the CFD code, not only with clean water, but also with sediment transport.

## References

- [1] Nosedà, G., Correnti permanenti con portata progressivamente decrescente, defluenti su griglie di fondo. *L'Energia Elettrica*, pp. 565-581, 1956.
- [2] Brunella, S., Hager, W. and Minor, H., Hydraulics of Bottom Rack Intake. *Journal of Hydraulic Engineering*, January, USA, pp. 4-9, 2003.
- [3] Righetti, M., Rigon, R. and Lanzoni, S., Indagine sperimentale del deflusso attraverso una griglia di fondo a barre longitudinali. Proc. of the XXVII Convegno di Idraulica e Costruzioni Idrauliche, 3, Genova, Italy, pp. 112-119, 2000.
- [4] Righetti, M. and Lanzoni, S., Experimental Study of the Flow Field over Bottom Intake Racks. *Journal of Hydraulic Engineering* © ASCE/ January pp. 15-22, 2008.
- [5] Orth, J., Chardonnet, E. and Meynardi, G., Étude de grilles pour prises d'eau du type. *La Houille Blanche*, 9(6), pp. 343-351, 1954.
- [6] Krochin, S. *Diseño Hidráulico*. Segunda Edición. Colección Escuela Politécnica Nacional. Quito. Ecuador, 1978.
- [7] Drobir, H., Entwurf von Wasserfassungen im Hochgebirge. *Österreichische Wasserwirtschaft*, Heft 11(12), 1981.
- [8] Castillo, L.G. and Lima, P., Análisis del dimensionamiento de la longitud de reja en una captación de fondo. *Proc. of the XXIV Congreso Latinoamericano de Hidráulica*, Punta del Este, Uruguay, 2010.
- [9] Yakhot, V. and Orszag, S.A., Renormalization group analysis of turbulence. I. Basic theory. *Journal of Scientific Computing*, 1(1), pp. 3-51, 1986.
- [10] Yakhot, V. and Smith, L.M., The renormalization group, the  $\varepsilon$ -expansion and derivation of turbulence models. *Journal of Scientific Computing*, 7(1), pp. 1, 1992.
- [11] FLOW 3D. FLOW Science, Inc., *FLOW 3D. Theory v10.0*, 2011.
- [12] Castillo, L. and Carrillo, J.M., Numerical simulation and validation of intake systems with CFD methodology. *Proc. of the 2nd IAHR European Congress*. Munich, Germany, 2012.

